Extra-Soft Self-Healable Supramolecular Silicone Elastomers from Bis-Amide-PDMS Multiblock Copolymers Prepared by Aza-Michael Reaction

Lucile Fauvre, Etienne Fleury, François Ganachaud, Daniel Portinha

Extra-soft self-healable supramolecular silicone elastomers from bis-amide-PDMS multiblock copolymers prepared by aza Michael reaction

Lucile Fauvre [δ], Etienne Fleury, François Ganachaud and Daniel Portinha*

Univ Lyon, CNRS, Université Claude Bernard Lyon 1, INSA Lyon, Université Jean Monnet, UMR 5223, Ingénierie des Matériaux Polymères, F-69621 Villeurbanne Cedex, France

[δ] Current address : Elkem Silicones France - ATRiON Research & Innovation Center, 9 rue Specia 69190 Saint-Fons, France

*Corresponding author: Daniel.portinha@insa-lyon.fr

Abstract

Silicone elastomers involving self-associating bis-amide groups were synthesized by aza-Michael addition between N,N'-methylenebis(acrylamide) and low molecular weight bis(3-aminopropyl)-terminated poly(dimethylsiloxane). In mild conditions that favour monoaddition (reaction of a primary amine) over diaddition (reaction of the resulting secondary amine), a library of non-cross-linked copolymers was prepared by tuning the (vinyl) to (primary amine) reactive functions molar ratio. Almost no diadduct was observed for reactive functions molar ratio lower than 0.8, leading thus to linear polymers with predictable molecular weights. On the other hand, diaddition occurs at higher molar ratios such that polymers with some branches, high molecular weights and large dispersity were synthesized. Whatever the polymers considered, the amide groups develop some H-bond interactions as demonstrated by FTIR, leading to phase-separated domains, as revealed by DSC, which alters rheological and viscoelastic properties of the polymers. By increasing the molecular weight of the polymers, it was shown possible to turn the copolymers from viscoelastic liquids to viscoelastic solids and further to elastomers. Moreover, the latter material presents self-healing propensity at room temperature, that may be related to the diffusion of short chains, while the mechanical properties (strain and stress at break) are endowed by the long entangled linear-like chains, properties that are recovered after healing.

Keywords

Aza Michael addition ; Silicone elastomer ; supramolecular interactions ; H-bonds ; self-healing

Introduction

Poly(dimethylsiloxane) (PDMS) and derivatives are of great interest due to their high flexibility, excellent thermal stability, hydrophobicity and biocompatibility[1], that make their corresponding elastomers essential in fields as versatile as biomaterials, sealants, joints or soft robotics[2,3]. Chemical (irreversible) crosslinking of these flexible chains, together with high loading of reinforcing silica fillers, lead to soft and resilient elastomer materials that present excellent performance in terms of high stretchability, good

self-recoverability and almost no creep. However, this technology goes along with reliability and sustainability concerns, as degradation and damages that are inflicted to the materials in one way or another during their use, are irreparable. In order to cope with these issues, developing re-organisable silicone networks has been the topics of intense studies for decades[4]. So-called self-mendable or self-healing PDMS-based materials are able to self-repair minor damage[5,6] with if possible full restoration of initial performance. Not only such networks meet the constraints of materials self-repair mentioned above, but they also open new perspectives in terms of processability and ways to reuse/recycle the materials at its end of life. From a structural point of view, such materials can be prepared by considering various strategies[7] such as the introduction of reversible covalent bonds[8-16], physical interactions[17-31], or a combination of the two[6, 32-35].

Regarding physical interactions, the introduction of supramolecular moieties in-between or along the PDMS chains that develop interactions together may result in phase-separated aggregates or crystalline domains in the PDMS matrix. The latter then act as robust physical crosslinks comparable to the chemical crosslinks in conventional elastomers, or the glassy and/or semi crystalline domains in thermoplastic elastomers, leading to the so-called thermoplastic silicone elastomers or TPSEs. In this context, a variety of non-covalent interactions has been proposed, such as hydrogen-bonding[6,17-19,] π-stacking[23-25], ionic pairing[28-30], metal-ligand association[20-22]. Tuning the strength of the interaction through chemical design or through an external stimulus, alters the connectivity of the physical network and can thus provide self-healing properties to silicone-based materials. This has in particular been shown with hydrogen bonding with numerous stickers of different strength. The overall strategy consists then in combining strongly interacting and weakly interacting groups within PDMS-based materials, such that the global supramolecular edifices weaken providing some dynamicity to otherwise solid TPSE materials[36]. For instance, reacting a bis-amino terminated PDMS with one symmetrical and another asymmetrical diisocyanate allowed tuning the strength of the H-bond interactions in the phase-separated domain of urea-based multiblock copolymers[37-38]. In other works, mixing bis-amino and bis-hydroxy-terminated PDMS with a symmetrical diisocyanate introduces strong (urea) and weak (urethane) associating groups that similarly allowed tuning the H-bond strength[39]. Another mean consists in adding to bis-urea-containing TPSEs, some monosubstituted urea-containing PDMS that were referred as 'stoppers'[40]. Another strategy, inspired by the work of Leibler et al on fatty acids[41], involves the use of urea with poly(amine) and/or poly(carboxylic acid) containing PDMS[42-46], which lead to numerous H-bonding groups such as amide, monoalkyl-urea, N,N – dialkylurea, imidazolidone. In all these reported works, the elastomers healed without any external stimulus at room temperature within few days. From a chemical point of view, the first type of reports[37-40] generally made use of bis-urea containing polymers or additives that involved the use of isocyanates, that raise severe health concerns in their proper synthesis or in their further use. The second type of reports[42-46] involved a two-steps process realized at high temperature that lead to different H-bonds groups, which content was difficult to control and which individual impacts on the supramolecular association and dynamicity are still unclear.

In this context, we turned to a simple and attractive chemical strategy that involves aza-Michael addition of amino-functional polysiloxane and N,N'-methylenebis(acrylamide) to obtain bis-amide-functionalized polysiloxane multiblock copolymers (scheme 1). We anticipated that the bis(β-aminoamide) linkers at the junction of PDMS segments would develop H-bonds and phase-separate from the silicone matrix, hopefully leading to TPSEs. By a simple step-growth addition, it is possible to tune the molecular weight and thus the average number of bis-amide groups per chain through the stoichiometry between the

reagents, as far as mono-addition of the primary (1°) amine onto the vinylic group that lead to a secondary (2°) amine is the only reaction (scheme 1a). Indeed, a primary amine used as a donor can undergo two consecutive Michael additions to an alkene, such that a 2° then a tertiary (3°) amine may result which would lead to branching and/or crosslinking if the extent of such reaction is important (scheme 1b).

Moreover, aza-Michael addition presents numerous complementary advantages including absence of any catalyst, mild reaction conditions, large panel of reactants available and no by-products. We have recently reviewed the potential of such reaction in silicon-containing molecules and polymers[47], in particular to prepare conventional chemical networks, but this reaction recently seen a revival of interest in the preparation of physically-crosslinked elastomer. For example, adenine and thymine nucleobase-functionalized polysiloxanes were synthesized by catalyst-free aza-Michael reaction in two steps and then mixed to prepare elastomers by a combination of homo and hetero self-assembly of the bases[48]. Later the same group reported the synthesis of non-covalent boron-nitrogen coordination bond mediated elastomer that repairs spontaneously and without external energy at room temperature[49]. In another work, a colourless, transparent, and healable PDMS-based elastomer was reported upon aza-Michael reaction of amino-siloxane and zinc acrylate and the resulting Zn(II)-carboxylate interactions[50]. Our group has recently reported the synthesis of zwitterionic silicone materials prepared by addition of acrylic acid onto amine-functional PDMS[51]. After a first instantaneous acid base reaction resulting in ionic pairs, aza-Michael reaction proceeded, leading to zwitterionic moieties that further assembled and phase separated in the silicone matrix.
The present work aims at studying the synthesis and supramolecular properties of bis-amide-containing multiblock silicones copolymers prepared by aza-Michael addition of N,N'-methylene bis-acrylamide on amino-functional polysiloxane. First, the synthesis and characterization of the polymers are described. Then, the rheological and viscoelastic properties of the obtained polymers are discussed. It is shown that for the amide-containing polymers of high molecular weight and a certain degree of branching, a viscoelastic solid like elastomer which presents self-healing propensity is obtained.

Experimental Part

Materials

All the reagents, hydrogenated and deuterated solvents were used as received without further purification. Fluid NH40d (Bis(3- aminopropyl) terminated PDMS, M_n = 3200 g/mol,**(1)**) was kindly provided by Wacker Chemie, Germany. DMS H25 (Hydride terminated PDMS, M_n = 17,200 g/mol, **(2)**) and DMS A32 (Bis(3-aminopropyl) terminated PDMS, M_n = 30,000 g/mol, **(3)**) were purchased from Gelest, USA.
N,N'-Methylenebis(acrylamide) (99%) was purchased from Sigma Aldrich. Common solvents such as tetrahydrofuran (≥ 99.9%), chloroform (99.9%) and isopropanol (≥ 99.9%) were purchased from Carlo Erba. Deuterated chloroform for NMR analyses ($CDCl_3$, 99.8%)) was purchased from Euriso-top.

Synthesis

In the following, the reactions were carried out with various molar ratios of acrylamide to amine functions. The reaction medium can be described by the feed composition denoted ***r'***, defined as the ratio of the molar amount of C=C bonds from the Michael acceptor, i.e. the bis-acrylamide, to the one of NH_2 from the Michael donor, i.e. the difunctional PDMS. This also corresponds to the molar ratio of the reactive groups when primary amines are involved in one Michael addition only. However, as a Michael

acceptor can react with either a 1° or a 2° amine, a 1° amine used as a donor can undergo two consecutive reactions; many published papers also introduce the molar ratio of reactive groups ***r*** defined as the ratio of the molar amount of C=C bonds to the molar amount of N-H bonds of a Michael donor.

$$\boldsymbol{r'} = \frac{\mathrm{n\,(C{=}C)}}{\mathrm{n}(\mathrm{N}H_2)} \text{ and } \boldsymbol{r} = \frac{\mathrm{n\,(C{=}C)}}{\mathrm{n}(\mathrm{N}H)} = \frac{\boldsymbol{r'}}{2}$$

In order to avoid crosslinking that might result from the double aza Michael addition on a primary amine or from the presence of residual double bonds in the final product according to an undesired reaction (facilitated upon heating for example), aza Michael reactions were conducted in order to totally consume the alkene groups and to favour the monoaddition, i.e. with ***r'***≤ 1.00 (***r***≤ 0.50).

In a typical example, N,N'-methylenebis(acrylamide) (0.125g, 0.81 mmol), polymer **(1)** (3.2g, 1 mmol) and isopropanol (1.7 mL, 22.6 mol) were mixed in a glass flask equipped with a stir bar, such that ***r'*** = 0.81 and the solvent content was 92.6 mol%. The reaction was conducted at different temperatures (room temperature or 50°C with the help of a hot plate) until completion of the reaction, that was monitored by ^{1}H NMR (a sample was then taken from the reaction medium, isopropanol totally removed under vacuum, at 50°C, and the crude product dissolved in deuterated chloroform). At the end of the reaction, the polymer was recovered by evaporation of solvent, then dried under vacuum at room temperature overnight.

Characterization methods

The determination of chemical structure was achieved by nuclear magnetic resonance (NMR) spectroscopy. ^{1}H NMR spectra were recorded on a Bruker Avance III 400 MHz apparatus while ^{13}C and 2D spectra were recorded on a Bruker Avance II 400 MHz Ascend apparatus. Samples were dissolved in $CDCl_3$ at room temperature and diluted enough (2 to 20 mmol/L) to avoid any residual physical association. Chemical shifts for ^{1}H NMR were determined in ppm downfield relative to residual $CHCl_3$ at δ_H = 7.26 ppm. Chemical shifts for ^{13}C NMR were quoted as ppm relative to the central peak of the $CDCl_3$ triplet
(δ_C = 77.23 ppm) as an internal standard.

FTIR spectra were recorded from the bulk using a Thermo Scientific Nicolet iS 10 spectrometer in transmission mode (KBr pellets) between 400 and 4000 cm^{-1}.

Size exclusion chromatography (SEC) was performed in THF on a Shimadzu apparatus with low masses separation mode. Three Waters gel columns were used, Styragel HR 0.5/1/2. THF was used as eluent, with a flow rate of 1 mL/min at 35°C (in an oven CTO-20A). Conventional calibration was set with polystyrene standards and molecular weights are expressed as PS equivalent. The detection was achieved by a Shimadzu RID 10-A differential refractometer.

Differential Scanning Calorimetry analyses were performed with a Q23 apparatus from TA Instrument, equipped with a Liquid Nitrogen Cooling System and using helium as inert gas. Samples were cooled down to -150°C (20°C/min), then heated up to 150°C (20°C/min) and this cycle was repeated once.

Rheological measurements were carried out on an ARES G2 apparatus. Frequency sweeps (0.1-15 Hz) were achieved at different temperatures and applied to cylindrical samples (~ 8 mm*1 mm). The master curves were constructed using isothermal dynamic frequency sweeps at 27.4 (reference temperature), 40, 60 and 80 ◦C by applying the time–temperature superposition (TTS) principle (horizontal shift).

Dynamic Mechanical Analyses were recorded onto a Mettler Toledo DMA SDTA861 apparatus, using the shear method on discoidal samples (6-8 mm*1.3-2.1 mm). The two discoidal samples were included in the shearing apparatus composed of two fixed parts at the extremities and one oscillating in the middle. Temperature sweeps were performed between -130 and 40°C, at 1 Hz, and 1% strain.

AFM characterizations were carried out on cryomicrotomed surfaces (-160°C), with a Dimension Veeco apparatus. Non-contact tips were used, of a 42 $N.m^{-1}$ spring constant (stiffness), with a resonance frequency around 330 kHz.

Tensile tests were carried out onto an MTS apparatus. Dogbone shaped specimens were made onto a 2 mm thick sheet with a cutting die H3, responding to the NFT 51-034 standards. The cutting die was soaked in liquid nitrogen prior to cutting. Pneumatic clamping jaw were used to maintain the sample, and 200 mm/min tensile rate was applied to the sample using a 10 N load cell. The self-healed samples were prepared by first cutting into two halves dog bone samples with a razor, then brought into close contact immediately while applying a small force and held together at 21°C for 72 hours.

Results and discussion

Polymer synthesis

In order to prepare bis-amide containing PDMS derivatives, we performed an aza-Michael addition between N,N'-methylenebis(acrylamide) (MBA) as the Michael acceptor with a low molecular weight bis(3- aminopropyl) terminated PDMS (polymer (**1**)) as Michael donor. As our objective was to prepare thermoplastic silicone elastomers, and not silicone rubber, it was important to work in conditions that favour the addition of the primary amine (1°) onto the alkene, referred as the monoaddition and that lead to a formed secondary amine (2°), and that limit the diaddition, related to the subsequent addition of the formed secondary amine onto an alkene that forms a tertiary amine (3°) (Scheme 1).

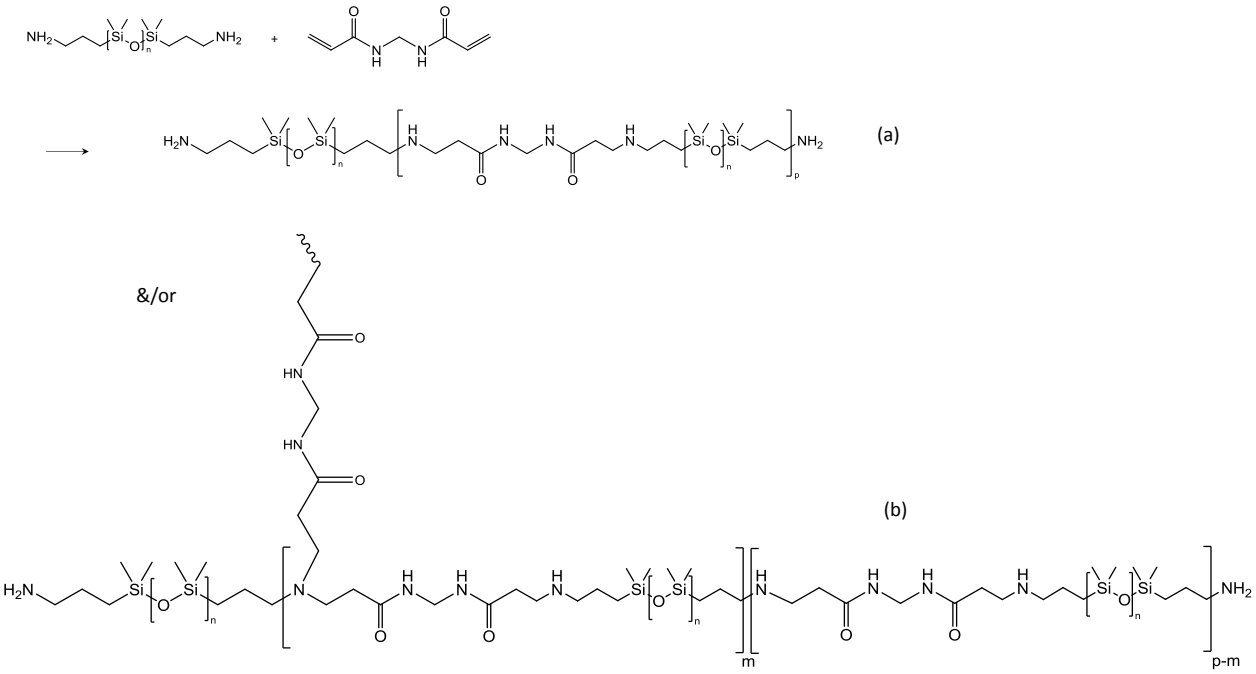

Scheme 1 – Aza-Michael addition of bis(3-aminopropyl)terminated PDMS to N,N'-methylenebis(acrylamide) with r' < 1 and possible products depending whether diaddition does not (a) or does (b) occur

In the meantime, another objective was to tune the molecular weight of the synthesized polymers that can be achieved by varying the feed ratio ***r'*** (with ***r'***< 1). As long as only one Michael addition occurs per primary amine group, the system would be assimilated to a step-growth polymerization with two difunctional reactants {A_2+B_2} which expected degree of polymerization DP_{th} at completion of the reaction can be calculated using the Carothers equation (eq. 1):

$$DP_{th} = \frac{1+r'}{1-r'} \qquad \text{(eq. 1)}$$

We have recently reviewed the impact of specific promoters or experimental conditions (polarity of solvent, feed ratio etc) on the features of the aza-Michael addition applied to silicon-based materials such as alkoxysilanes and polysiloxanes[47]. In particular, the use of base and acid catalysts to activate the Michael donor and acceptor respectively, were reported but they often induced undesired side products or needed harsh conditions. [52,53] Other catalysts were reported, such as heterogeneous polymer-supported catalyst[48] or graphene oxide[54] but their use might be irrelevant when intending to prepare solid-like materials as they would remain in the sample. While aza Michael reaction can be carried out without any solvent, our group has reported a complete study on how the type and nature of solvent and reactive groups molar ratio ***r'*** could be tuned not only to favour one or the other adduct, but also to favourably play on the reaction kinetics for aza Michael reactions involving acrylates and amino-PDMS[55]. For example, we have shown that working in isopropanol with reactive ratios ***r'*** □ 1.0 at RT led to a complete consumption of the alkene functions after 48 hours with a monoadduct (MA) content around 96 mol.% with less than 2 mol% of diadduct (DA). Increasing the temperature to 95°C led to a complete reaction after 6 h without affecting significantly its selectivity.

Back to the current study, a screening of the operating conditions was first realized. As MBA is a solid with a limited miscibility with amino-terminated PDMS, aza-Michael reactions have to be carried out in a solvent in conditions that favour the synthesis of the MA (one addition of a primary amine onto an alkene) with a total consumption of the alkene groups; this is to prevent the presence of residual C=C as chain ends on the final polymer to avoid any subsequent reaction upon storage with the 2° amines available along the backbone. To verify these two conditions and as an illustration, we first discuss the results obtained with a ratio ***r'*** □ 0.81 (r □ 0.41) in isopropanol (92.6 mol.%). The reaction was monitored by ^{1}H NMR on a sample taken from the reaction mixture. In particular, completion of the reaction is attested by the absence of the three signals in the [5.5 – 6.5] ppm range ascribed to the vinylic protons of acrylamide groups (see Figure S1). For the preceding conditions, these peaks were vanished after one week, showing that the reaction is slower than the one conducted with butyl acrylate in similar conditions[55] (see Figure S2). While Michael reactions involving silicon-based materials were mostly conducted at room temperature, working at elevated temperature is an easy means to accelerate the reactions[56-57], having in mind that too high temperatures should be avoided to limit retro-additions[47]. Back to our system, increasing temperature to 50°C actually accelerates the reaction which was completed after 48h (data not shown). These operating conditions (50°C, in isopropanol, 92.6 mol.%) were thus applied to different feed compositions with ***r'*** ≤ 1 (***r'*** = 0.53, 0.71, 0.81, 0.90, 0.96, □ 1.0), to tune the molecular weight of the resulting polymers while keeping the same end chains. The resulting polymers were isolated, then characterized by ^{1}H NMR which lead to two categories of samples based on

this analysis. We focused the description of the resulting ^{1}H NMR spectrum in the [2.0 – 3.0] ppm range that is very sensitive to the chemical environment of 1°, 2° and 3° amines that may be encountered in Aza-Michael additions (Figure 1).

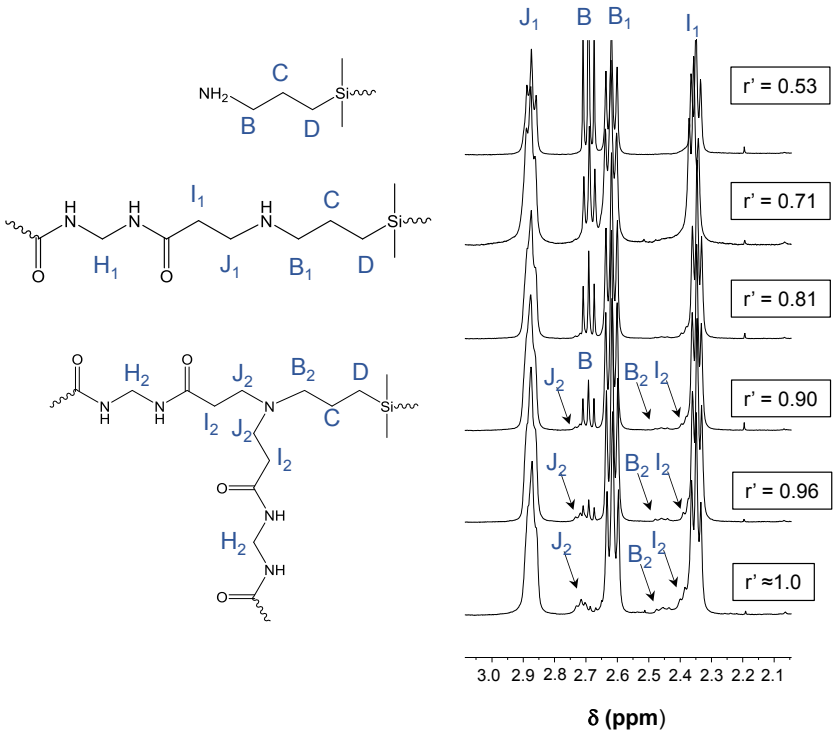

Figure 1: Zoom in the [2.0 – 3.0] ppm range of ^{1}H NMR spectra obtained for isolated polymers synthesized using various *r'* values, and respective assignment of the peaks

For ***r'*** ≤ 0.71, the spectra reveal signals at δ = 2.85 ppm (signal J_1) and 2.32 ppm (signal I_1), characteristics of the methylene groups at the α and β positions of the 1° amine that result from the reaction of the acrylamide monomer, and at δ = 2.60 ppm (signal B_1) ascribed to the methylene group at the α position of the 1° amine that arise from the PDMS macromonomer, respectively. One can also notice the presence of a peak at δ = 4.55 ppm (signal H_1), ascribed to the methylene group besides the amide groups (see Figure S2). The proportionality between the integrals of the peaks ($I_{I_1} \sim I_{J_1} \sim I_{B_1} \sim 2I_{H_1}$) in conjunction with the absence of any other noticeable peak, tend to show that only monoaddition has occurred. As the reaction reached completion of the alkene function in default, the signal at δ = 2.66 ppm is ascribed to the methylene group in α position of a 1° amine function that acts as a chain end (signal B). One can thus calculate the experimental degree of polymerization DP_{exp} determined by ^{1}H NMR using the following equation:

$$DP_{exp} = \frac{I_B + 2I_{B_1}}{I_B} \qquad \text{(eq. 2)}$$

For the samples where ***r'*** ≥ 0.81, the ^{1}HNMR spectra of the isolated sample reveal an ill-defined peak at δ = 2.44 ppm, as well as a peak emerging to the left foot of the peak at δ = 2.32 ppm ascribed to I_1. An additional peak (at δ = 2.70 ppm) that partially overlaps the well-distinguishable triple ascribed to B at δ

= 2.66 ppm is also visible. Moreover, the proportionality expected between the integrals of the signals at δ = 4.55 ppm, 2.85 ppm, 2.60 and 2.32 ppm if only 2° amine was present is not verified anymore, confirming that new peaks are superimposed to the previously identified ones. These peaks are ascribed to the methylene groups in α position (J_2 and B_2) and in β position (I_2) of the 3° amine, in agreement with our previous study that reported the selectivity of acrylates towards primary amino-PDMS[55], and finally attest that diaddition has occurred. As this stage, it is important to note that the samples are macroscopically soluble in various samples such as chloroform or THF, and thus that no visible crosslinking has occurred. This agrees with what is observed in systems which monomers own multiple functions with very different reactivity, and which has been used to prepare hyperbranched polymers (HBPs) through aza-Michael additions in more cost-effective, straightforward one-pot processes than the stringent conditions needed when monomers with equal reactivity are used[58]. However, as a result of the occurrence of diaddition, branched polymers are obtained. For such polymers, structural units are classified as dendritic unit D (associated to the presence of a 3° amine), linear unit L (associated to the presence of a 2° amine), and terminal unit T (associated to the presence of a primary amine), and the degree of branching DB[59], that indicates the branching structure of the polymer, is consequently defined by:

$$DB = \frac{T+D}{T+L+D} \qquad \text{(eq.3)}$$

For a dendrimer that corresponds to a perfectly branched polymer, there is no L unit, and DB = 1 (100%). As L units are considered as structural defects for dendrimers, when their number increases, the structure evolve towards a hyperbranched polymer, then a branched polymer, then a linear polymer. DB depends on many factors, including the structure and the functionality of the monomer(s), the chemical strategy that is developed, the polymerization conditions etc[55]. For example, Hawker et al. reported the polymerization of AB_2, AB_3 and AB_4 monomers composed of the same subunit to form hyperbranched poly(ether ketone)s.[61] The DB of a polymer obtained from an AB_4 monomer was 71%, whereas polymerization of an AB_2 monomer yielded a DB of 49%. The latter value agrees with the one expected theoretically for an ideal statistical self-condensation of an AB_2 monomer, which means equal reactivity of all B groups and no side reactions.[62] It should also be noted that HBPs mays possess many isomers for the same DB such that it is challenging to ascertain the exact topology; for example, even if DB is equal to 100%, self-condensation of AB_2 monomer may appear as a quasi-linear polymer, as a dendrimer wedge or a hyperbranched polymer. Despite this difficulty, it is agreed that for a given chemical strategy, the polymer evolves towards a less branched structure as DB decreases.

For polymers with some branching, structural characteristics DP and DB could be quantified by ^{1}H NMR using the integrals of signals B, B_1 and B_2. However, contrary to the case of our previously reported acrylate adducts[55], the signals ascribed to B is superimposed with J_2, and B_2 peak, which integral is small, is really closed to the superimposed signals of I_1 and I_2. Indeed, the signal of the methylene groups (I_1) and (J_2) are less deshielded as the carbonyl in an amide is much less electronegative than a carbonyl of an ester group is, because of the resonance of the nitrogen in the amide function.
Taking into account the proportionality between the integrals of signals I_1, J_1 and B_1 ($I_{I_1} = I_{J_1} = I_{B_1}$) and signals B_2, I_2 and J_2 ($I_{I_2} = I_{J_2} = 2I_{B_2}$), values for the integrals of B can be calculated from the integrals of the {B + J_2} and B_2 peaks, respectively. Before going further, we determined the 1°, 2° and 3° amine composition with these integral values. For the sample with ***r'*** □ 1, composition of 3.2%, 95% and 2.0% were found, respectively (see Table S1). These values are in good agreement with those reported for the butyl acrylate/amino PDMS system under comparable solvent conditions and molar composition[55]. Values of $DP_{\text{exp, branched}}$ and DB_{exp} can then be calculated according to the following equations:

$$DP_{exp,\ branched} = \frac{I_B + 2I_{B_1} + 3I_{B_2}}{I_B - I_{B_2}} = \frac{I_{B+J_2} + 2I_{B_1} + I_{B_2}}{I_{B+J_2)} - 3I_{B_2}} \quad \text{(eq. 4)}$$

$$DB_{exp} = \frac{I_{B_1} + I_{B_2}}{I_B + I_{B_1} + I_{B_2}} = \frac{2I_{(I_1+I_2+B_2)} - 2I_{J_1}}{I_{B+J_2} - 3I_{B_2}} \quad \text{(eq. 5)}$$

The degree of polymerization for each sample was calculated according to equations (2) and (4) depending on whether or not the NMR spectra show the additional peaks. For sample with ***r'*** = 0.81, as the NMR signals related to 3° amine are very weak, the DP was calculated according to both equations. All the results are gathered in Table 1.

Table 1: Feed composition, theoretical (according to (equ. 1)) and experimental DP for corresponding polymers (thanks to ^{1}H NMR). When the peaks ascribed to 3° amine were observed, experimental DP were calculated using (eq 4). Experiments carried out in isopropanol (92.6 mol.%) at 50°C except for * (40°C).

Polymer	*r'*	$DP_{,th}$	DP_{exp} (almost no 3° amine)	$DP_{exp,\ branched}$ (3° amine detected)	DB_{exp}
(4)	0.53	3.3	3.4	/	
(5)	0.71	6.1	6.6	/	
(6)*	0.81	9.8	11	12	0.17
(7)	0.90	19	/	22	0.11
(8)	0.96	49	/	68	0.06
(9)	□1.00	/	/	145	0.05

For samples with ***r'*** ≤ 0,71, signals of 3° amine are hardly visible and the samples can thus be considered as purely linear. In this case, the experimental degree of polymerization is in good agreement with the one predicted by using eq. 1, attesting that linear polymers with tuneable molecular weights can be prepared. When ***r'*** ≥ 0.81, the signals ascribed to the 3° amine are visible, attesting that some diaddition occurred. We had reported such trend on our study on the Michael addition of butyl acrylate onto amino-terminated PDMS, even in conditions that favoured the synthesis of the MA[55]. The resulting polymers own a DP that deviates more and more from the predicted value obtained by the Carothers equation for {A_2+B_2} system as ***r'*** increases; in the meantime, the degree of branching is getting smaller and smaller as ***r'*** increases, with a DB of 0.05 for ***r'*** □ 1, suggesting that on average this polymer presents a limited number of branching per chain.

To highlight the impact of such structural differences, some samples were analysed by SEC realized in THF; Figure 2 presents the chromatograms obtained for polymer **(6)** – rather linear- and **(9)** – which own some branching points.

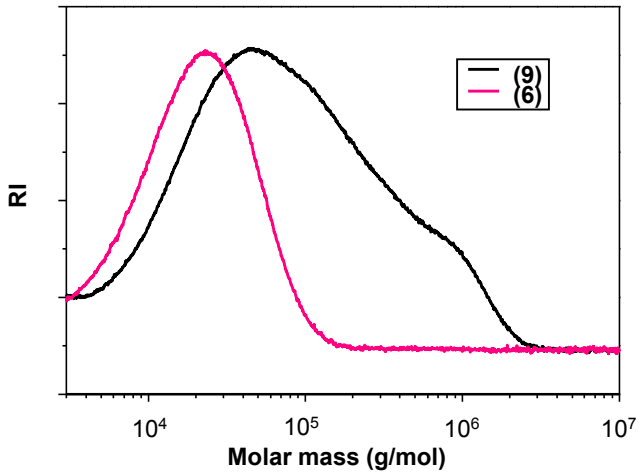

Figure 2 : SEC traces in THF for polymers (6) and (9).

Besides the fact that their molar masses are very different (M_n = 13 kg.mol^{-1} and 34.6 kg.mol^{-1} for polymers **(6)** and **(9)**, respectively), as expected when changing ***r'***, the most striking point concerns the difference in dispersity between the two polymers. Indeed, sample **(6)** exhibits a dispersity of Đ = 2.1 (M_w = 27 kg.mol^{-1}), close to the expected value for linear polymers synthesized by step-growth polymerization, in agreement with the degrees of polymerization calculated either with (eq. 2) and (eq. 4) considering the polymer either as linear or with some branches. On the contrary, polymer **(9)** exhibits a very large dispersity of Đ = 5.7 (M_w □ 196 kg.mol^{-1}), in agreement with what is generally observed for branched polymers[60]. Many parameters can explain this very large dispersity, related to structural (number, length of branches being either linear or tree-like, etc.) or compositional factors (mixture of linear and branched chains etc.); at this stage, we can retain that the sample **(9)** presents a very broad range of molar masses which can have an important effect on the properties of the polymer (*vide infra*).

Supramolecular associations

The bis-amide containing PDMSs synthesized here may develop hydrogen bonds, and solid-state FTIR spectroscopic analyses were conducted to confirm it. Spectra were recorded upon heating from room temperature up to 160 °C and then upon cooling down to room temperature. Herein are reported the results for polymer **(6)** (Figure 3). We particularly focused on the N-H stretching vibration (3500-3100 cm^{-1}) and amide vibration (amide I and amide II vibrations, 1750-1450 cm^{-1}). The sample initially presents some water probably trapped in the polar groups of the sample, as confirmed by a large peak at 3450 cm^{-1} for the spectrum recorded at room temperature. This peak largely decreases upon heating and does not reappear upon cooling, as a consequence of evaporation, which allows easier observation of the peaks' shift upon cooling. Before heating, two peaks are visible at room temperature, one centered at 3200 cm^{-1}, and another one at 3280 cm^{-1}. The latter one is assigned to N-H bonds in amide groups that interacts through H-bonds. Upon heating, this peak is shifted to 3325 cm^{-1} in conjunction with a decrease of intensity. According to literature, this hypsochromic shift is associated to the decrease of the hydrogen bond strength, while intensity decrease and peak shift are both due to the increase of the distance between interacting groups and to a higher mobility[63]. In the meantime, a small peak at 3450 cm^{-1}, assigned to free N-H bonds in amide functions, appears upon heating; moreover, upon cooling, its intensity decreases. All these observations show that hydrogen-bonded N-H groups are

present at room temperature, that part of them tends to dissociate upon heating while some other remains but are getting weaker. Regarding the peak at 3200 cm^{-1}, it was assigned to hydrogen-bonded NH of amine groups which content decreases upon heating and rises again upon cooling. This peak is all the more visible that this sample owns a low molecular weight (see Table 1). Regarding the second domain of interest, the amide I mode (mainly the C=O stretching vibration) also presents a hypsochromic shift (1663 cm^{-1} to 1676 cm^{-1}) upon heating, assigned to the disorganization of hydrogen bonds at higher temperature. One peak at 1700 cm^{-1} associated to free carbonyl groups, was expected at higher temperature, but cannot be seen as the peak centered at 1676 cm^{-1} is too broad. For the amide II mode (mainly the N-H in plane bending vibration), a bathochromic shift was observed (1545 cm^{-1} to 1520 cm^{-1}) as expected when decreasing hydrogen bond strength, together with a decrease of the intensity. Signal of unbonded amide was expected at 1500 cm^{-1}, and such a peak appears as a shoulder at high temperature. All these results confirm that the polymer develop hydrogen bonds involving the amide groups at room temperature, and that the intensity of such interactions are decreased when increasing temperature. Noteworthy, all polymers described in Table 1 present comparable results.

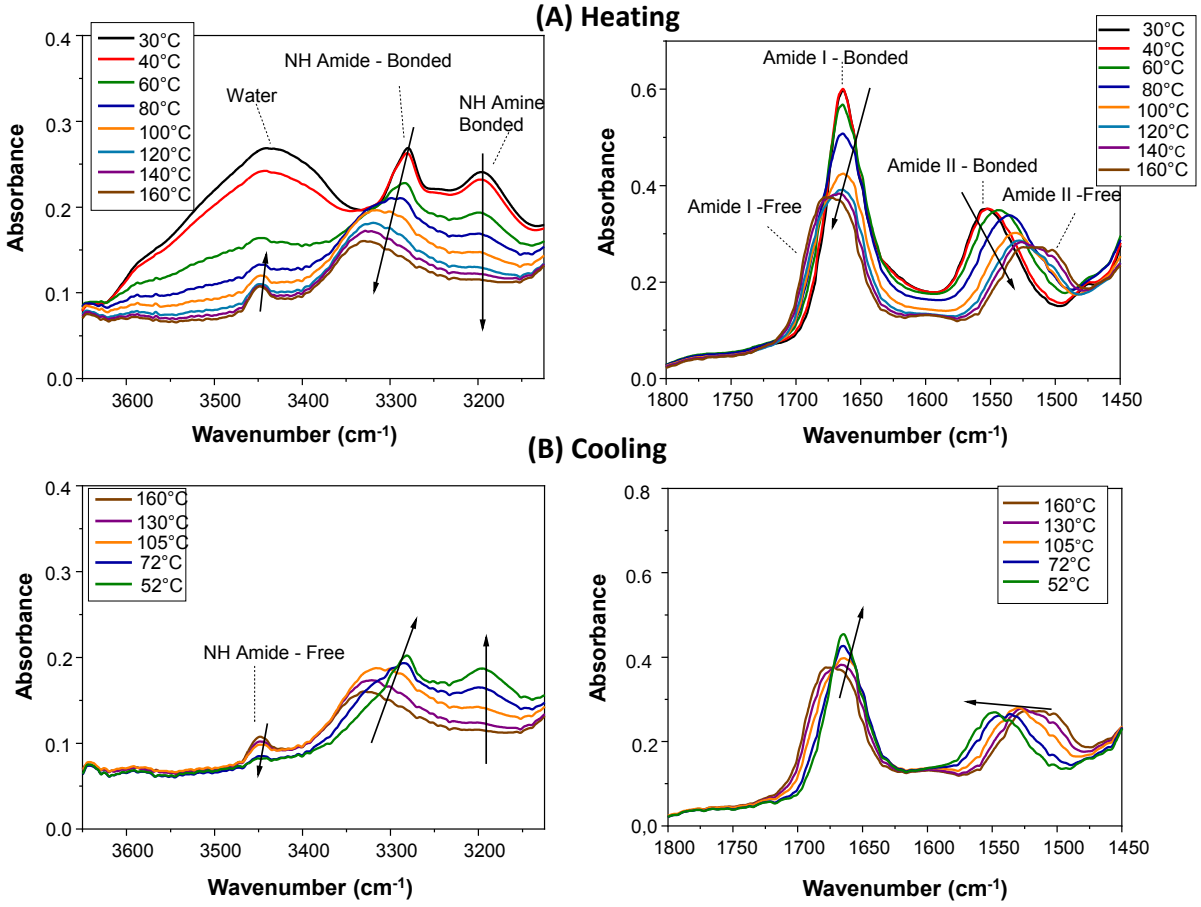

Figure 3 : Zoom of the FTIR spectra of polymer (6) during the heating process (A) and cooling process (B)

About thermal properties, differential scanning calorimetry (DSC) confirmed that the initial PDMS presents only one glass transition temperature (Tg) at around – 123°C and neither a melting nor crystallization transitions, in agreement with its low molecular weight (data not shown). Regarding the

bis-amide-containing polymers, they all display two transitions, one glass transition temperature at -120°C and another wide transition that starts at -40°C for all the samples (See Figure S3). These are associated to transitions that occur in the PDMS matrix and in the bis-amide containing organic domains that are not miscible together. This is often observed for PDMS-based materials modified with very polar groups able to develop supramolecular interactions such as hydrogen bonding[24] or ionic bonds[51]. AFM was conducted on this polymer to investigate whether an organization of the material was detected, but no phase separation could be observed regardless of the magnification used (see Figure S4). Thus, the phase separated domains which were envisaged by DSC results, were too small and/or not well-ordered enough to be detected.

Viscoelastic behaviour

The rheological behaviour of all copolymers is now discussed in terms of the complex viscosity as a function of the frequency at room temperature. For a matter of comparison, the results obtained for commercially available PDMS samples with close molecular weights (polymers **(1)**, **(2)** and **(3)**) but without any bis-amide groups are also presented. For polymers **(1)** to **(3)**, their complex viscosity is constant with the frequency and the value increases with molecular weight. Two significant differences appear for bis-amide containing polymers **(6)** to **(9)**: (i) their complex viscosity is much higher than the commercial ones, despite comparable molecular weights for some of them, and (ii) they all show a non-Newtonian behaviour with a complex viscosity that depends on the frequency. For polymer **(6)**, the complex viscosity value measured at f = 5Hz is about 200 larger than the one of hydride-terminated PDMS (**2**) with comparable molecular weights. As the average molecular weight value is lower than the critical molecular weight value for which entanglements are encountered for PDMS (24,500 $g.mol^{-1}$)[64], physical interactions between chains through hydrogen bonds involving the amide groups are responsible for such phenomenon.

For the other samples which molecular weight is larger than the critical one, both the increase in complex viscosity (i.e. 500 times larger for polymer **(7)**, than for its commercial counterpart polymer **(3)**), and the frequency-dependence are more pronounced. This can be the results of combined effect of higher average molecular weight that favours entanglements, and number of bis-amide groups per chain that may increase the number of physical crosslinks through hydrogen-bonding per chains. In the measured frequency range, all the bis-amide containing polymers present some viscoelastic properties with a frequency-thinning behaviour. It is well-known that branched polymers exhibit various rheological behaviour as a function of their degree of branching, topology etc[60]. In particular, when their DB is high, they behave as Newtonian fluids while they show a frequency-dependent thinning behaviour when they bear short and/or only few branches. Regarding polymer **(9)** that presented some branches as determined by ^{1}H NMR, the frequency-dependence behaviour of the complex viscosity shows that it can undergo polymer chain entanglement, attesting that it owns a nearly linear-like structure as confirmed by the low DB that was calculated.

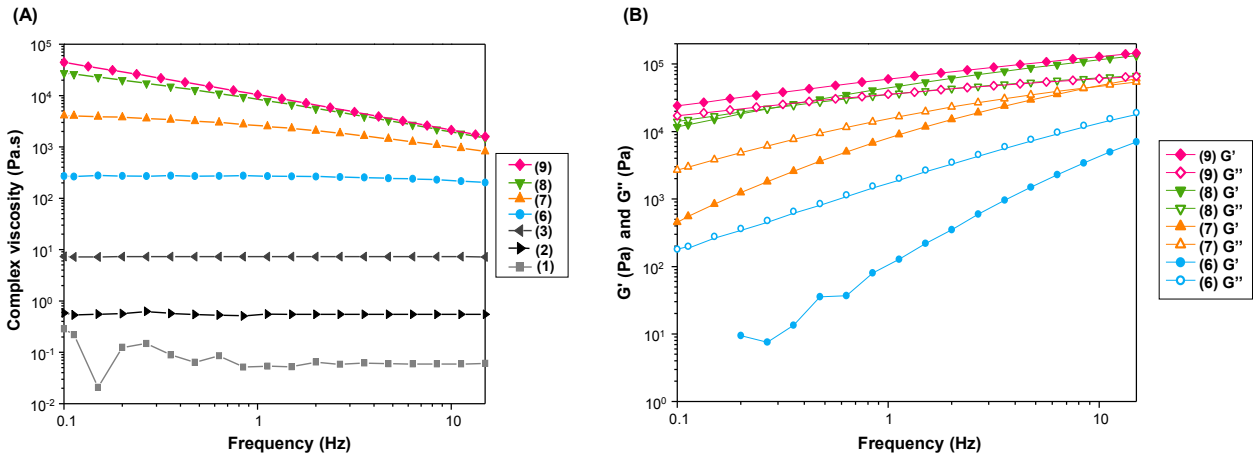

Figure 4: A) Complex viscosity modulus as a function of frequency for bis-amide free commercially available products and for bis-amide containing polymers prepared by aza-Michael. B) Storage (*G*', full symbols) and loss (*G*'', empty symbols)) moduli versus frequency of bis-amide containing polymers (see Table 1).

Macroscopically speaking, a significant change in the polymer state was also observed when increasing the molecular weight of the bis-amide containing samples. To highlight this, the viscoelastic data are provided by plotting the storage (G') and loss (G'') moduli as functions of frequency (Figure 4B). For sample polymer **(6)**, with low molecular weight, *G*'' remains higher than *G*' over the entire frequency range confirming that the product behaves as a viscous liquid. Conversely to the complex viscosity, the moduli are getting less dependent upon the frequency when the molecular weight of the samples are increased, which confirms that the samples exhibit viscoelastic properties. Starting from a liquid with viscoelastic properties over the frequency range, a crossover between *G*' and *G*'' is observed when increasing molecular weights of the bis-amide containing polymers (at $f \approx$ 10Hz for polymer **(7)**, at $f \approx$ 0.3Hz for polymer **(8)**. For polymer **(9)**, with the highest molecular weight, a viscoelastic solid material is revealed as *G*' > *G*'' over the whole frequency range.

In the next part we focus the study on polymer **(9)**. The time-temperature superposition principle was first applied to plot a master curve obtained by sweeping frequencies at different temperatures (Figure 5A). The storage modulus is higher than the loss modulus over the whole range of frequencies (more than four decades). At intermediate frequencies, the storage modulus and the loss modulus are very close and evolve in a similar way, following the same power law $G' \alpha G'' \alpha \omega^n$ with n~0.4. When this power law is observed over the entire range of frequency for polymers that are able to chemically[65] or physically[66] crosslink, the polymer is at the gel point and referred to as a "critical gel"[67]. However, for polymer **(9)**, when the frequency lowers, the storage modulus deviates and moves away from the loss modulus which slope remains constant. This result shows that our sample is somehow close to but has passed the gel point and behaves as a soft viscoelastic solid.

Mechanical properties of solid material and self-healing

Dynamic mechanical analyses as a function of temperature were further carried out on polymer **(9)**. With relatively weak viscoelastic properties the shear mode was the most adapted one. The evolution of storage and loss moduli as a function of the temperature sweep between -130°C and 40°C, at 1 Hz frequency and 1% strain are shown (Figure 5B). At the beginning of the analysis, the viscoelastic solid is glassy, with a plateau $G' = 2*10^2$ MPa until $T_\alpha \approx$ -110°C. A rubbery plateau was observed between -80°C and -30°C, attesting the elastomer-like behaviour which structure does not evolve significantly with

temperature. The storage modulus of this polymer at the plateau is around 0.4 MPa. Neither a melting or a crystallization transitions appeared, confirming the DSC results. From -30°C, a decrease in *G*' and a dispersion maximum in *G*'' are observed. This indicates a higher mobility in the sample upon heating, that may be somehow ascribed to a decrease in the H-bond strength with the experimental time that would exceeds the lifetime of the physical crosslinks in the supramolecular network. We also notice that *G*' is still larger than *G*'' at least until 40°C, which attests that the polymer does not flow at room temperature. Considering the range of temperature, this means that the sample might be self-adaptable at a temperature close to the ambient one, and may present some self-healing properties.

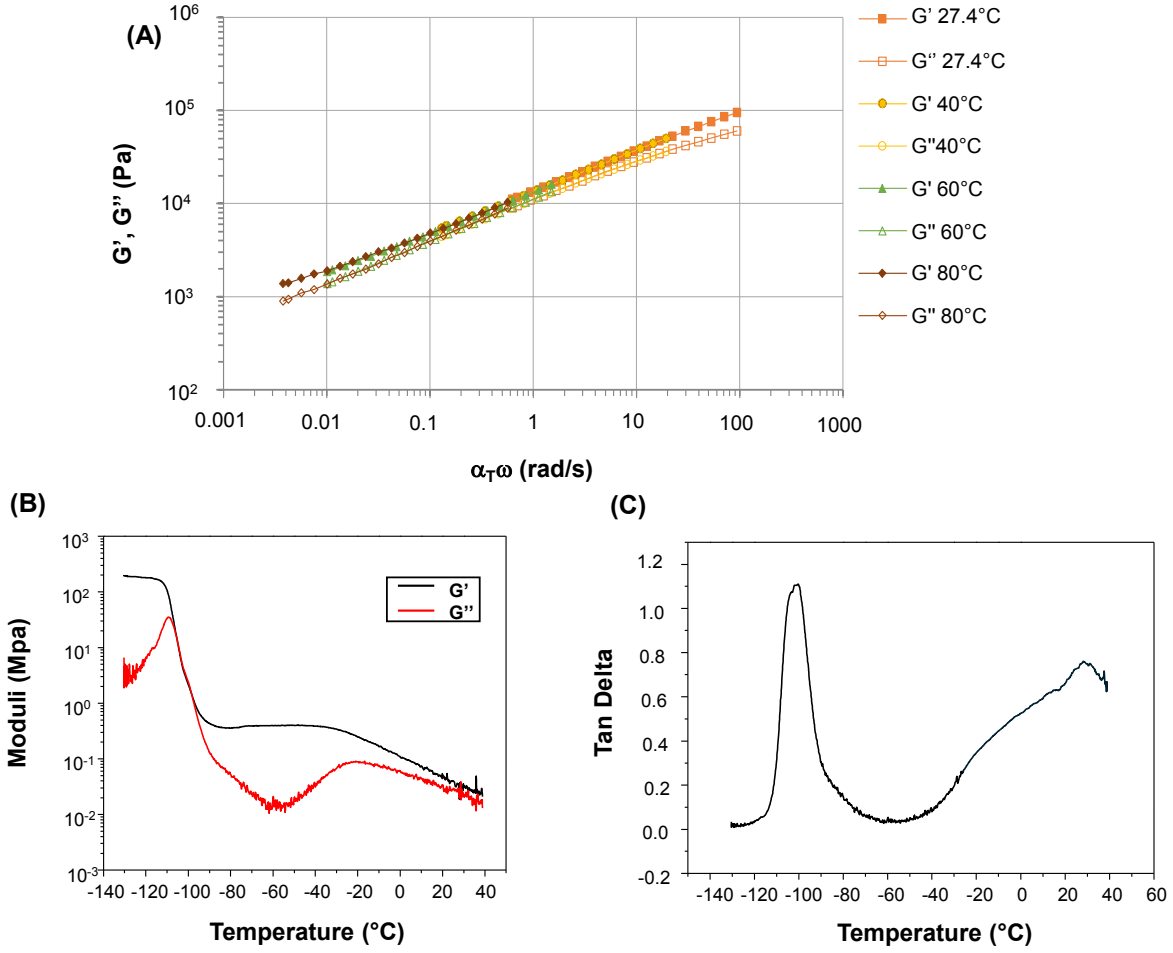

Figure 5: A) Viscoelastic properties through Time-Temperature Superposition plot for polymer (9). Temperature of reference is 27.4°C. Rheological measurements were carried out at 1% strain, from 27.4 to 80°C. Polymer is solid over the whole range of frequencies (G'>G'') B) Storage (G') and Loss(G'') moduli and C) tan (δ) versus temperature for polymer (9) (1 Hz frequency, 1% strain)

To prove this, mechanical properties of product (**9**) were compared for pristine and healed specimens. The latter were prepared by first cutting into two halves dog bone samples with a razor that were then brought into close contact immediately while applying a small force and held together at 21°C for 72 hours. Mechanical properties were determined by uniaxial tensile tests on two independent samples for each product (Figure 6A). When comparing the results for pristine samples together, we observe a

somehow large error when carrying these tests, that we assign to the weak mechanical properties of the sample and the difficulties to get a specimen without any defaults. The same behaviour was observed for healed samples. Considering this, we observe a fair strain for the samples larger than 1500%, with a full recovery of both stress and strain for the healed sample when compared to the pristine sample (Figure 6). The values of ultimate tensile strength of the samples (0.1 MPa) are also similar with each other, and also comparable to that observed for a conventional soft chemically cross-linked silicone elastomer[68-69]. Considering that the dispersity of polymer **(9)** is large, we ascribe the large strain of the samples to entanglements ensured by the chains with high molecular weights, much larger than the critical molecular weight between entanglements for PDMS, and to the hydrogen-bonded groups that contributes to physically crosslink chains together. In the meantime, the self-healing propensity is ensured by the other part of the sample associated with chains of lower molecular weights, that can more easily move in the bulk but cannot flow as a result of the H-bonds.

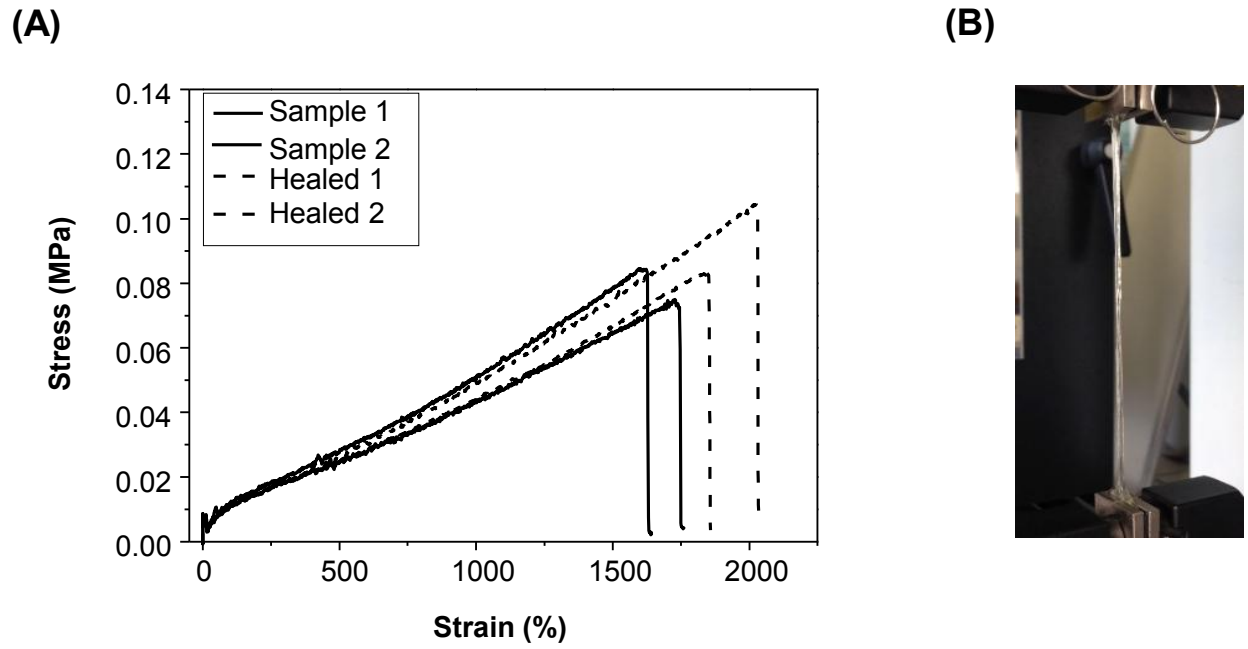

Figure 6 A) Nominal stress-strain profiles for pristine and healed samples of polymer (9) (healing at 21°C for 72 hours) B) Picture of one healed sample during tensile test.

Conclusion

This article has detailed the preparation of bis-amide containing silicone-based polymers synthesized through aza-Michael reaction of N,N'-methylenebis(acrylamide) (MBA) with α, ω amino-terminated PDMS of low molecular weight . By tuning the (alkene) to (1° amine) molar ratio in a solvent that favours the monoaddition, non-crosslinked polymers were prepared in smooth conditions. For low value of ***r'***, linear polymers with predictable molecular weights and expected dispersity could be prepared by considering the reaction as a $\{A_2+B_2\}$ step-growth polymerization. For higher values of ***r'***, diaddition occurs that lead to polymers with some branches, higher molecular weight and large dispersity as expected when branching occurs. Structural parameters were determined by ^{1}H NMR and SEC. All samples showed rheological properties that are higher than the ones of commercially available amide-free PDMS samples with comparable molecular weights, demonstrating the influence of amide groups that interact through hydrogen-bonding, as confirmed by FTIR studies. Two thermal transitions were

revealed by DSC analyses, one ascribed to the silicon-based phase and a second one with a wide-temperature range from -40°C up to 40°C (at least). As regards of structural parameters, when the molecular weight of the polymer was lower than the critical molecular weight between entanglements reported for PDMS, the polymers behaved as a viscoelastic liquid while when the molecular weight increased above the critical value, an elastomer-like PDMS based material was obtained. Thus, as the samples present a frequency-dependent behaviour typical of polymers that can undergo entanglement, diaddition has contributed to increase molecular weight and to widen dispersity while the polymer own a rather linear-like structure. Moreover, the solid-like material presented some self-healing propensity at room temperature. This may be the result of the combined effects of the presence of Hydrogen-bonded groups with somehow low association ability (either in terms of strength and/or stacking/aggregation) which may provide the sample with high dynamicity: while the presence of low molecular chains endowed the sample with high mobility, longer chains maintained the solid-like property without any terminal flow. This will be more discussed in a forthcoming paper that will specifically address these points while introducing some fillers in the formulation.

Supporting Information

The Supporting Information is available free of charge at https://pubs.acs.org/doi/10.1021/xxxxxxxxxxxxxxxx :

^{1}H NMR spectra of crude product with r' = 0.81 at 27% and full conversion, respectively; integrals of relevant signal observed by ^{1}H NMR spectra and determination of the composition in 1°, 2° and 3° amine thereof; DSC thermograms for polymers **(6)** and **(9)**; AFM micrographs for polymer **(9)** at two distinct magnitudes (PDF).

Acknowledgements

The authors thanks Dr Guillaume Falco (MateIS, INSA-Lyon) for the AFM analysis. The authors gratefully acknowledge the NMR Polymer Center at "Institut de Chimie de Lyon" (FR 203) for the access to NMR facilities. This work has benefited from the facilities and expertise of the Liquid Chromatography Platform (Institut de Chimie de Lyon) for the characterization of polymers.

Financial support

The authors acknowledge the financial support from Agence Nationale de la Recherche (ARCADE – Grant # 15-CE08-0022).

Conflict of interest

The authors declare that they have no conflict of interest.

TOC graph

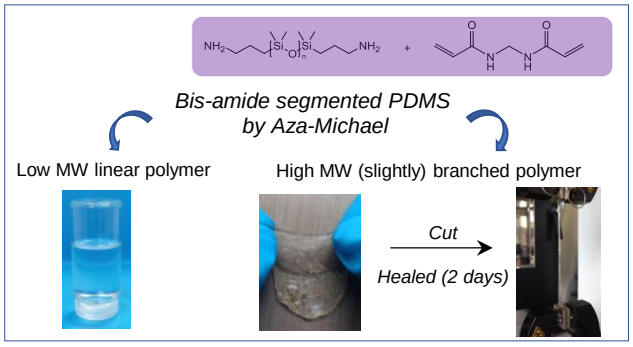

References

1. Yilgör, E.; Yilgör, I. Silicone Containing Copolymers: Synthesis, Properties and Applications, Prog. Polym. Sci. 2014, 39, 1165-1195.
2. Mi, Y.; Chan, Y.; Trau, D.; Huang, P.; Chen, E. Micromolding of PDMS Scaffolds and Microwells for Tissue Culture and Cell Patterning: A new Method of Microfabrication by the Self-Assembled Micropatterns of Diblock Copolymer Micelles Polymer, 2006, 47, 5124-5130.
3. Whitesides, G. M. Soft Robotics Angew. Chem., Int. Ed. 2018, 2-18.
4. Wang, Z. ; Lu, X. ; Sun, S. ; Yu, C. ; Xia, H. J. Mater. Chem. B, 2019, 7, 4876-4926.
5. Pena-Francesch, A.; Jung, H.; Demirel, M. C.; Sitti, M. Biosynthetic Self-Healing Materials for Soft Machines Nat. Mater. 2020, 19, 1230−1235.
6. Guo, H.; Han, Y.; Zhao, W.; Yang, J.; Zhang, L. Universally Autonomous Self-Healing Elastomer with High Stretchability Nat. Commun. 2020, 11, 2037-2045.
7. Fauvre, L.; Portinha, D.; Fleury, E.; Ganachaud, F. Thermoplastic Silicone Elastomers as Materials Exhibiting High Mechanical Properties and/or Self-Healing Propensity J Adhes. Sci. Technol. 2021, 35, 2723-2735.
8. El-Zaatari, B. M.; Ishibashi, J. S. A.; Kalow, J. A. Cross-Linker Control of Vitrimer Flow Polym. Chem. 2020, 11, 5339-5345.
9. Sun, J.; Pu, X.; Liu, M.; Yu, A.; Du, C.; Zhai, J.; Hu, W.; Wang, Z. L. Self-Healable, Stretchable, Transparent Triboelectric Nanogenerators as Soft Power Sources ACS Nano 2018, 12, 6147-6155.
10. Bui, R.; Brook, M. A. Catalyst Free Silicone Sealants That Cure Underwater Adv. Funct. Mater. 2020, 30, 2000737.
11. Kathan, M.; Kovaricek, P.; Jurissek, C.; Senf, A.; Dallmann, A.; Thunemann, A. F.; Hecht, S. Control of Imine Exchange Kinetics with Photoswitches to Modulate Self-Healing in Polysiloxane Networks by Light Illumination Angew. Chem., Int. Ed. 2016, 55, 13882-13886.
12. Lai, J.-C.; Mei, J.-F.; Jia, X.-Y.; Li, C.-H.; You, X.-Z.; Bao, Z. A Stiff and Healable Polymer Based on Dynamic-Covalent Boroxine Bonds Adv. Mater. 2016, 28, 8277-8282.
13. Lossada, F.; Guo, J.; Jiao, D.; Groeer, S.; Bourgeat-Lami, E.; Montarnal, D.; Walther, A. Vitrimer Chemistry Meets Cellulose Nanofibrils: Bioinspired Nanopapers with High Water Resistance and Strong Adhesion Biomacromolecules 2019, 20, 1045-1055.
14. Tran, T. N.; Rawstron, E.; Bourgeat-Lami, E.; Montarnal, D. Formation of Cross-Linked Films from Immiscible Precursors through Sintering of Vitrimer Nanoparticles ACS Macro Lett. 2018, 7, 376-380.

15. Tang, M.; Zheng, P.; Wang, K.; Qin, Y.; Jiang, Y.; Cheng, Y.; Li, Z.; Wu, L. Autonomous Self-Healing, Self-Adhesive, Highly Conductive Composites Based on a Silver-Filled Polyborosiloxane/Polydimethylsiloxane Double-Network Elastomer J. Mater. Chem. A 2019, 7, 27278-27288.
16. Zheng, P.; McCarthy, T. J. A Surprise from 1954: Siloxane Equilibration is a Simple, Robust, and Obvious Polymer Self-Healing Mechanism J. Am. Chem. Soc. 2012, 134, 2024-2027.
17. Liu, M.; Liu, P.; Lu, G.; Xu, Z.; Yao, X. Multiphase-Assembly of Siloxane Oligomers with Improved Mechanical Strength and Water-Enhanced Healing Angew. Chem., Int. Ed. 2018, 57,11242-246.
18. Xu, J.; Chen, P.; Wu, J.; Hu, P.; Fu, Y.; Jiang, W.; Fu, J. Notch-Insensitive, Ultrastretchable, Efficient Self-Healing Supramolecular Polymers Constructed from Multiphase Active Hydrogen Bonds for Electronic Applications Chem. Mater. 2019, 31, 7951-7961.
19. Ma, X.; Zhou, D.; Liu, L.; Wang, L.; Yu, H.; Li, L.; Feng, S. Reprocessable Supramolecular Elastomers of Poly(Siloxane–Urethane) via Self-Complementary Quadruple Hydrogen Bonding Macromol. Chem. Phys. 2021, 222, 2100116.
20. Oh, J. Y.; Son, D.; Katsumata, T.; Lee, Y.; Kim, Y.; Lopez, J., Wu, H.-C.; Kang, J.; Park, J.; Gu, X.; Mun, J., Wang, N. G. J.; Yin, Y.; Cai, W.; Yun, Y.; Tok, J. B.-H.; Bao, Z. Stretchable Self-Healable Semiconducting Polymer Film for Active-Matrix Strain-Sensing Array Sci. Adv. 2019, 5, eaav3097.
21. Mo, J.; Wu, W.; Shan, S.; Wu, X.; Li, D.; Li, R.; Lin, Y.; Zhang A. A Systematic Study on Zn(II)-Iminocarboxyl Complexation Applied in Supramolecular PDMS Networks Polymer, 2022, 250, 124896.
22. Zhao, P.; Wang, L.; Xie, L.; Wang, W.; Wang, L.; Zhang, C.; Li, L.; Feng, S. Mechanically Strong, Autonomous Self-Healing, and Fully Recyclable Silicone Coordination Elastomers with Unique Photoluminescent Properties Macromol. Rapid Commun. 2021, 42, 2100519.
23. Fawcett, A. S.; Brook, M. A. Thermoplastic Silicone Elastomers through Self-Association of Pendant Coumarin Groups Macromolecules 2014, 47, 1656-1663.
24. Liu W.-X.; Liu, D.; Xiao, Y.; Zou, M.; Shi, L.-Y.; Yang, K.-K.; Wang, Y.-Z. Healable, Recyclable, and High-Stretchable Polydimethylsiloxane Elastomer Based on Synergistic Effects of Multiple Supramolecular Interactions Macromol. Mater. Eng. 2022, 307, 2200310.
25. Mei, J.-F. ; Jia, X.-Y.; Lai, J.-C.; Sun, Y.; Li, C.-H.; Wu, J.-H.; Cao, Y.; You, X.-Z.; Bao, Z. A Highly Stretchable and Autonomous Self-Healing Polymer Based on Combination of Pt···Pt and π–π Interactions Macromol. Rapid Commun. 2016, 37, 1667-1675.
26. Miwa, Y.; Taira, K.; Kurachi, J.; Udagawa, T.; Kutsumizu, S. A Gas-Plastic Elastomer that Quickly Self-Heals Damage with the Aid of CO_2 Gas Nat. Commun., 2019, 10, 1828-1833.
27. Bossion, A.; Olazabal, I.; Aguirresarobe, R. H.; Marina, S.; Martin, V.; Irusta, L.; Taton, D.; Sardon, H. Synthesis of Self-Healable Waterborne Isocyanate-Free Poly(hydroxyurethane)-Based Supramolecular Networks by Ionic Interactions Polym. Chem. 2019, 10, 2723-2733.
28. Shi, J.; Zhao, N.; Yan, D.; Song, J.; Fu, W.; Li, Z. Design of a Mechanically Strong and Highly Stretchable Thermoplastic Silicone Elastomer Based on Coulombic Interactions J. Mater. Chem. A 2020, 8, 5943-5951.
29. Lu, H.; Feng, S. Supramolecular Silicone Elastomers with Healable and Hydrophobic Properties Crosslinked by "Salt-Forming Vulcanization" J. Polym. Sci., Part A: Polym. Chem. 2017, 55, 903-911.
30. Mo J.; Chen, X.; Fu Y.; Li R.; Lin Y.; Zhang A. A Solvent-Free, Transparent, Self-Healing Polysiloxanes Elastomer Based on Unsaturated Carboxyl-Amino Ionic Hydrogen Bonds Polymer 2021, 228, 123903.

31. Fu, R.; Zhang, J.; Liu, S.; Xu, X.-D.; Feng, S. Facile Construction of a Double Network Cross-Linked Luminescent Supramolecular Elastomer by Hydrosilylation and Pillar[5]arene Host–Guest Recognition Chem. Commun. 2020, 56, 6719-6722.
32. Li, J.; Niu, H.; Yu, Y.; Gao, Y.; Wu, Q.; Wang, F.; Sun, P. Supramolecular Polydimethylsiloxane Elastomer with Enhanced Mechanical Properties and Self-Healing Ability Engineered by Synergetic Dynamic Bonds ACS Appl. Polym. Mater. 2021, 3, 3373-3382.
33. Dai, S. ; Li, M.; Yan, H.; Zhu, H.; Hu, H.; Zhang, Y.; Cheng, G.; Yuan, N.; Ding, J. Self-Healing Silicone Elastomer with Stable and High Adhesion in Harsh Environments Langmuir 2021, 37, 13696-13702.
34. Chen, G.; Wen, S.; Yue, Z. Design of Robust Self-Healing Silicone Elastomers Based on Multiple H-Bonding and Dynamic Covalent Bond Langmuir 2022, 38, 1194–1203.
35. Zhang, K., Wang, Z.; Zhang, J.; Liu, Y.; Yan, C.; Hu, T; Gao, C., Wu, Y. A Highly Stretchable and Room Temperature Autonomous Self-Healing Supramolecular Organosilicon Elastomer with Hyperbranched Structure Eur. Polym. J. 2021, 156, 110618.
36. Lamers, B.A.G.; Sleczkowsli, M. L.; Wouters, F.; Engels, T. A. P.; Meijer, E. W.; Palmans, A. R. A. Tuning Polymer Properties of Non-Covalent Crosslinked PDMS by Varying Supramolecular Interaction Strength Polym. Chem. 2020, 11, 2847-2854.
37. Kang, J.; Son, D.; Wang, G. J. N.; Liu, Y.; Lopez, J.; Kim, Y.; Oh, J. Y.; Katsumata, T.; Mun, J.; Lee, Y.; Jin, L.; Tok, J. B.-H.; Bao, Z. Tough and Water-Insensitive Self-Healing Elastomer for Robust Electronic Skin Adv. Mater. 2018, 30, 1706846.
38. Döhler, D. ; Kang, J. ; Cooper, C. B.; Tok, J. B.-H.; Rupp, H.; Binder, W. H.; Bao, Z. Tuning the Self-Healing Response of Poly(dimethylsiloxane)-Based Elastomers ACS Appl. Polym. Mater. 2020, 2, 4127–4139.
39. Chen, H.; Koh, J. J.; Liu, M.; Li, P.; Fan, X.; Liu, S.; Yeo, J. C. C.; Tan, Y.; Tee, B. C. K.; He, C. Super Tough and Self-Healable Poly(dimethylsiloxane) Elastomer via Hydrogen Bonding Association and Its Applications as Triboelectric Nanogenerators ACS Appl. Mater. Interfaces 2020, 12, 31975–31983.
40. Simonin, L.; Falco, G.; Pensec, S.; Dalmas, F.; Chenal, J.-M.; Ganachaud, F.; Marcellan, A.; Chazeau, L.; Bouteiller, L. Macromolecular Additives to Turn a Thermoplastic Elastomer into a Self-Healing Material Macromolecules 2021, 54, 888–895.
41. Cordier, P.; Tournilhac, F.; Soulié-Ziakovic, C.; Leibler, L. Self-Healing and Thermoreversible Rubber from Supramolecular Assembly Nature 2008, 451, 977–980.
42. Zhang, A.; Yang, L.; Lin, Y.; Yan, L.; Lu, H.; Wang, L. Self-Healing Elastomers Based on the Multi-Hydrogen Bonding of Low-Molecular Polydimethylsiloxanes: Synthesis and Characterization J. Appl. Polym. Sci. 2013, 129, 2435-2442.
43. Zhang, A.; Deng, W; Lin, Y.; Ye, J.; Dong, Y.; Lei, Y.; Chen, H. Novel Supramolecular Elastomer Films Based on Linear Carboxyl-Terminated Polydimethylsiloxane Oligomers: Preparation, Characterization, Biocompatibility, and Application in Wound Dressings J. Biomater. Sci., Polym. Ed. 2014, 25, 1346–1361.
44. Yang, L.; Lin, Y.; Wang, L.; Zhang, A. The Synthesis and Characterization of Supramolecular Elastomers Based on Linear Carboxyl-Terminated Polydimethylsiloxane Oligomers Polym. Chem. 2014, 5, 153-160.
45. Cao, P.-F.; Li, B.; Hong, T.; Townsend, J.; Qiang, Z.; Xing, K.; Vogiatzis, K. D.; Wang, Y.; Mays, J. W.; Sokolov, A. P.; Saito, T. Superstretchable, Self-Healing Polymeric Elastomers with Tunable Properties Adv. Funct. Mater. 2018, 1800741.
46. You, Y.; Zhang, A.; Lin, Y. Crosslinking Mechanism of Supramolecular Elastomers Based on Linear Bifunctional Polydimethylsiloxane Oligomers J. Appl. Polym. Sci. 2016, 133, 43385.

47. Genest, A.; Portinha, D.; Fleury, E.; Ganachaud, F. The Aza-Michael Reaction as an Alternative Strategy to Generate Advanced Silicon-Based (Macro)molecules and Materials Prog. Polym. Sci. 2017, 72, 61-110.
48. Cao, J.; Feng L.; Feng, S. Preparation of Supramolecular Silicone Elastomers *via* Homo- and Hetero-Assembly New J. Chem. 2018, 42, 1973-1978.
49. Cao, J.; Han, D.; Lu, H.; Zhang, P.; Feng, S. A Readily Self-Healing and Recyclable Silicone Elastomer via Boron–Nitrogen Noncovalent Crosslinking New J. Chem. 2018, 42, 18517-18520.
50. Bai, L.; Qv, P.; Zheng, J. Colorless, Transparent, and Healable Silicone Elastomers by Introducing Zn(II)–Carboxylate Interactions via Aza-Michael Reaction J. Mater. Sci. 2020, 55, 14045-14057.
51. Genest, A.; Portinha, D.; Pouget, E.; Lamnawar, K.; Ganachaud, F.; Fleury, E. Zwitterionic Silicone Materials Derived from Aza-Michael Reaction of Amino-Functional PDMS with Acrylic Acid Macromol. Rapid Comm. 2021, 42, 2000372.
52. Azizi, N.; Baghi, R.; Ghafuri, H.; Bolourtchian, M.; Hashemi, M. Silicon Tetrachloride Catalyzed Aza-Michael Addition of Amines to Conjugated Alkenes under Solvent-Free Conditions Synlett, 2010, 3, 379–382.
53. Rulev, A. Y. Aza-Michael Reaction: Achievements and Prospects Russ. Chem. Rev. 2011, 80, 197–218.
54. Verma, S.; Mungse, H. P.; Kumar, N.; Choudhary, S.; Jain, S. L.; Sain, B.; Khatri, O. P. Graphene Oxide: an Efficient and Reusable Carbocatalyst for Aza-Michael Addition of Amines to Activated Alkenes Chem. Commun. 2011, 47, 12673–12675.
55. Genest, A.; Binauld, S.; Pouget, E.; Ganachaud, F.; Fleury, E.; Portinha, D. Going Beyond the Barriers of Aza-Michael Reactions: Controlling the Selectivity of Acrylates Towards Primary Amino-PDMS Polym. Chem. 2017, 8, 624–630.
56. Zintchenko, A.; van der Aa, L. J.; Engbersen, J. F. J. Improved Synthesis Strategy of Poly(amidoamine)s for Biomedical Applications: Catalysis by '"Green"' Biocompatible Earth Alkaline Metal Salts Macromol. Rapid Commun. 2011, 32, 321–325.
57. Tang, X.-J.; Yan, Z.-L.; Chen, W.-L.; Gao, Y.-R.; Mao, S.; Zhang, Y.-L.; Wang, Y.-Q. Aza-Michael Reaction Promoted by Aqueous Sodium Carbonate Solution Tetrahedron Lett. 2013, 54, 2669–2673.
58. Wu, D.; Liu, Y.; Chen, L.; He, C.; Shung Chung, T.; Goh, S. H. $2A_2$+ BB'B'' Approach to Hyperbranched Poly(amino ester)s Macromolecules 2005, 38, 5519-5525.
59. Hawker, C.J.; Lee, R.; Fréchet, J. M. J. One-Step Synthesis of Hyperbranched Dendritic Polyesters J. Am. Chem. Soc. 1991, 113, 4583-4588.
60. Voit, B. I.; Lederer, A. Hyperbranched and Highly Branched Polymer Architectures – Synthetic Strategies and Major Characterization Techniques Chem. Rev. 2009, 109, 5924-5973.
61. Hawker, C. J.; Chu, F. Hyperbranched Poly(ether ketones): Manipulation of Structure and Physical Properties Macromolecules 1996, 29, 4370-4380.
62. Hölter, D.; Burgath, A.; Frey, H. Degree of Branching in Hyperbranched Polymers, Acta Polym. 1997, 48, 30–35.
63. Woodward, P. J.; Merino, D. H.; Greenland, B. W.; Hamley, I. W.; Light, Z.; Slark, A. T.; Hayes, W. Hydrogen Bonded Supramolecular Elastomers: Correlating Hydrogen Bonding Strength with Morphology and Rheology Macromolecules 2010, 43, 2512–2517.
64. Clarson, S. J.; Semlyen, J. A. Siloxane Polymers, Englewood Cliffs, N.J.: Prentice Hall, 1993.
65. Chambon, F.; Winter, H. H. Linear Viscoelasticity at the Gel Point of a Crosslinking PDMS with Imbalanced Stoichiometry J. Rheol. 1987, 31, 683–697.
66. Cuvelier, G.; Launay, B. Frequency Dependence of Viscoelastic Properties of some Physical Gels near the Gel Point Makromol. Chem., Macromol. Symp. 1990, 40, 23–31.
67. Winter, H. H. The Critical Gel. In *Structure and Dynamics of Polymer and Colloidal Systems*; Borsali,

R.; Pecora, R. Eds.; Springer, 2011, pp.439-470.
68. Bueche, A. M. The Curing of Silicone Rubber with Benzoyl Peroxide J. Polym. Sci. 1955, 15, 105–120.
69. Yuan, Q. W.; Mark, J. E. Reinforcement of Poly(dimethylsiloxane) Networks by Blended and *In-Situ* Generated Silica Fillers Having Various Sizes, Size Distributions, and Modified Surfaces Macromol. Chem. Phys. 1999, 200, 206–220.